

Structure and Dynamics of Indonesian H274Y Mutant Avian Influenza Virus Neuraminidase Type 1 (N1) with Its Inhibitors

Sigit Jaya Herlambang⁺ and Rosari Saleh

Department of Physics, Math and Science Faculty, University of Indonesia / Jl. Margonda Raya Depok, Jawa Barat, 16424, Indonesia

Abstract. The purpose of this research was to confirm the ability of zanamivir (ZA) and laninamivir (LA) to inhibit H274Y mutant using heating dynamics simulation. To accomplish that, the homology modeling and models assessments, the best model (model 3) was selected and used for molecular docking, and heating dynamics simulation were completed. The trajectories were analyzed using root mean square deviation (RMSD), the percentage of hydrogen bonds occupancy between NA and its inhibitors, and free binding energies comparison. The results shows the highest and fluctuating NA-oseltamivir carboxylate (NA-OS) RMSD compared with other inhibitors, the larger numbers of residues which formed strong hydrogen bonds and the lower free binding energies of LA and ZA compared with peramivir (PE) and oseltamivir carboxylate (OS). This occurrence indicated that the interaction between NA-ZA and NA-LA is better than in NA-OS and NA-PE complexes which correlated with the ability of ZA and LA to treat OS-resistant NA.

Keywords: neuraminidase, inhibitor, homology modeling, docking, heating dynamics

1. Introduction

The latest update of H5N1 outbreak was happened in backyard poultry in Banteay Meanchey province, Cambodia which had been reported to the World Health Organization (WHO) in 12 September 2011 [01]. Since the early event of highly pathogenic avian influenza (HPAI) H5N1 virus in 1996, the localized outbreaks are continuously occurred in many countries with an economical background in poultry farming. As one of the countries mentioned before, Indonesia also was impacted as a result of pandemics. The H5N1 virus has spread over poultries in 31 of 33 provinces and 12 of provinces were reported hundreds cases of human infection [02]. As of October 2011, 179 cases occurred with 147 deaths reported in cumulative number of confirmed human cases for avian influenza A H5N1 reported to WHO in the years between 2003-2011 [03]. Until now, Indonesia becomes the country with the most human deaths surpassing Vietnam and Egypt.

Continuously outbreaks give a sign that the H5N1 virus is still have a potential to produce the next, higher mortality, and larger outbreak which could becomes an epidemic. Thus, routine and continued surveillance is needed in several places known as the potentially infected such as poultry farm and its markets. In the influenza report, Ortrud Werner and Timm C Harder wrote that, over the years, the virulence of H5N1 for mammals has increased and the host range has expanded [04]. It had been reported that H5N1 in China from 1999 to 2002, and in Vietnam since 2003 have become progressively more pathogenic for mammals [05]. Furthermore, Georg Behrens and Matthias Stoll define two qualities of influenza account for much of the epidemiological spread of the virus. First, is the ability to emerge and circulate in avian or porcine reservoirs by either genetic re-assortment or direct transmission and subsequently spread to humans at irregular intervals. Second, is the fast and unpredictable antigenic change (drift and shift) of important

⁺ Corresponding author. Tel.: +6287882840959; Fax: +62-751-51-71
E-mail address: sigit.jaya.herlambang@gmail.com

immune targets once the virus has become established in a human [06]. However, the transmission process is the key of global spread of H5N1 [07].

The transmission process of virus depends on its both glycoproteins, hemagglutinin (HA) and neuraminidase (NA), which is also play a role in replication [08]. The HA molecule bind the sialic acid (SA) as a receptor and induces penetration to host cell while NA molecule cleaved SA to detach matured virion from the host cell. A single mutation in one of those two glycoproteins can lead into resistance against its inhibitors. Several studies about inhibitors-resistant virus were explained a few specific NA residues, such as R292K, H274Y, R152K, E119V, and N294S, which created huge impact in tamiflu treatment [09-19]. Furthermore, OS-resistant in H274Y mutant had been reported to be caused by the reorientation of the adjacent E276 forcing its carboxyl group to move closer to the binding site [09, 20]. But it only happened until researcher found an alternative compounds to be a promising competitor of SA in binding with the mutant NA [21-23]. Their experiments suggest ZA and LA to solve OS-resistant virus problem.

In this study we report comparative Indonesian NA structure models and its dynamics when interacted with four inhibitors, ZA, LA, PE, and OS. The main objective of this study is to compare the interactions between NA and inhibitors when heated with heating dynamics simulation. Even this simulation is way too short to reveal conformational changes, but in this timescale is sufficient to observed atoms in the active site and its interaction with inhibitors.

2. Materials and Methods

2.1. Template Selection and Sequence Alignment

The amino acid sequence of H274Y mutant NA type 1 (N1) from the HPAI virus (A/Indonesia/560H/2006(H5N1)) was obtained from National Center of Biotechnology Information (NCBI) [24] with the accession code ABW06159. The 449 residues long sequence was used to identify homologous sequences with BLASTP 2.2.16 [25] and InterProScan [26] provided by Swiss Expasy [27-31]. The most homologous template, with greatest similarity sequence, resulted was a crystal structure with protein data bank code 3CKZ taken from Research Collaboratory for Structural Bioinformatics (RCSB) [32].

2.2. Homology Modeling and Models Assessments

Five models were generated using build homology modeling which utilize MODELER [33]. The parameters of optimization level was set into medium and cut overhangs added to remove the terminal unaligned residues in models. All models were evaluated to verify its reliability with Discrete Optimized Protein Energy (DOPE) method [34] using MODELER and 3D-profiles [35, 36]. The parameter for MODELER was set with DOPE-HR method, which is very similar to the DOPE method but obtained at high resolution. The parameter for 3D-profiles was set with smooth windows sized 10 and Kabsch-Sander algorithm for secondary structure method [37]. All models were sent to Swiss Expasy to be analyzed with PROCHECK [38-40] to get insight the stereochemical properties of the models using Ramachandran plot.

2.3. Molecular Docking

The structures of inhibitors were collected in the database of chemical molecules, PubChem [41] which is maintained by NCBI. At this moment, PubChem provide over 31 millions compounds, 75 millions substances and bioactivity results from 1644 high-throughput screening programs. Until this time, there were 13 NA inhibitor compounds, but only four inhibitors had been used in this simulation: ZA, PE, OS, and LA.

The attachment of inhibitors into NA molecule has completed with CDOCKER [42]. The parameters set with 10 random top hits and conformations, 1000 random conformations dynamics steps and conformations dynamics target temperature, including electrostatic interactions and orientation van der Waals energy threshold, and use CHARMM [43-44] for forcefield and ligand partial charge. The candidate poses were created using random rigid-body with six degrees of freedom (3 rotations/3 translations) followed by simulated annealing. Sphere generated to fill the active site to facilitate ligand matching in the sphere centre and find possible ligand orientations. Following that, a final minimization used to refine the ligand process. A pose with minimum interaction energy would be ranked in the top of 10 random top hits.

2.4. Minimization Energy

The best docked pose have a large energy gradient, 13,000 kcal/(mol x Å). A proper energy minimization is needed in order to produce an optimum geometrical structure. The energy minimization process was divided by two main steps with different algorithms, steepest descent and conjugate gradient. The steepest descent was executed with targeted energy gradient 0.5 kcal/(mol x Å) and 1,000,000 steps maximum. The second step was executed with targeted energy gradient 0.1 kcal/ (mol x Å) and 1,000,000 steps maximum. Both methods use Generalized Born Molecular Volume (GBMV) implicit solvent energy to mimicking the aqueous environment [45], SHAKE algorithm [46], a non bond list radius of 14 Å, and a switching function was applied between 10-12 Å for a computational efficiency [47-48]. To gain a long-range electrostatic energy contribution, it was visualized in a spherical cutoff mode.

2.5. Heating Dynamics Simulation

Heating dynamics simulation was executed with 100 picosecond (ps) time simulation. All systems temperature rose from 0 into 300 K with the parameters used were 50,000 steps, 2 femtosecond (fs) time step, and the trajectory data were stored every 0.1 ps. Other parameters such as GBMV, SHAKE algorithm, non bond list radius, and switching function were set identical with minimization energy.

Calculation of the ligand-receptor complex was based on the equation below:

$$\bar{G} = \bar{E}_{MM} + \bar{G}_{solvation} - TS \quad (1)$$

\bar{G} is the average Gibbs energy, $\bar{G}_{solvation}$ is the electrostatic and nonpolar free energy from implicit solvation. In this particular study, GBMV was applied for implicit solvation minimization energy and heating dynamics only. For free binding energies, the calculation was done in vacuum. The last term (TS) is the temperature and entropy contribution, while the first term of the right hand side (\bar{E}_{MM}) is the energy term produced by the applied forcefield, which is the potential energy of the system [49]:

$$E_{MM} = E_{potential} = E_{bond} + E_{angle} + E_{torsion} + E_{out\ of\ plane} + E_{electrostatic} + E_{vanderWaals} \quad (2)$$

The relationship between the ligand, receptor, and complex energy is given in the next equation:

$$\Delta G_{binding} = \bar{G}_{complex} - \left(\bar{G}_{ligand} + \bar{G}_{receptor} \right) \quad (3)$$

The (1) equation is average Gibbs energy which constructed each component energy in the (3) equation. Furthermore, all phases of the study described in this section from structure preparation to heating dynamics simulation were conducted with Discovery Studio 2.1 (Accelrys).

3. Results

3.1. Structures preparation

The five homology models were generated with homology modeling from 3CKZ template. All models had been refined and renumbered since the 3CKZ template has a few broken peptide bonds and there are also repeated numbers such as 169 and 169-A residues, 345 and 345-A, and 412, 412-A, 412-B, 412-C and 412-D. Repeated numbers does not mean there are two residues in one position, but only the next residue has numbered, with the same number and the alphabetical addition after the number, as its previous position residue.

The models and template were assessed with three different methods and the results are shown in the table 1. The verify scores of all models varies from 192-201 which is higher than the high expected score, 175.54. The highest score was occupied by model 3 which being the only one model who exceed template score. Second assessment using DOPE-HR scores that relate with the stability of molecules. The more high DOPE-HR score indicated the worst model and should not be taken for simulation. All DOPE score of the structures assessed are varies in range -36,386 to -34,793 and had satisfied the spatial restraints. The lowest DOPE-HR score of structures assessed is template 3CKZ. The comparison without template show that model

3 which have the lowest DOPE-HR score. The result from PROCHECK provides Ramachandran plots of all NA residues without glycine and proline. In the table 1, the PROCHECK data shown is the percentage of NA residues which in the most favoured and additionally allowed regions. The template is taking the first place with 99.7% followed by model 3 and 4 with 99.4%. All assessment methods being used in this experiment are in agreement that the model 3 is the best NA model compared with other models generated.

Table 1: The Assessment Scores of 5 Homology Models.

Template and Models	Verify Score	DOPE	Most Favoured& Additional Residues Percentage (without Gly and Pro)
Model 1	192.99	-35183	98.8%
Model 2	198.73	-34793	99.1%
Model 3	200.3	-36386	99.4%
Model 4	197.4	-35510	99.4%
Model 5	197.98	-35311	99.1%
Template 3CKZ	199.53	-42594	99.7%

3.2. Molecular Docking and Energy Minimization

The model 3 as the best model was subjected to molecular docking with four inhibitors mentioned before. Each NA-inhibitor molecular docking process has conferred 10 poses. A pose with the smallest CDOCKER energy was used to create a complex. After being docked, steepest descent and conjugate gradient energy minimization were executed. The hydrogen bonds formed between NA-inhibitor before and after minimizations were observed. The increasing numbers of hydrogen bonds formed between NA-inhibitor happened in the interaction between NA and ZA, and between NA and LA. In NA-ZA complex, the numbers of the hydrogen bonds formed increase from 11 to 13 while in NA-LA is from 9 to 10. The 6 hydrogen bonds formed in NA-OS complex is constant while in NA-PE precisely decreased from 7 to 6. However, the minimization process resulting in satisfied energy gradient of all complex structures and brought all complexes total energies into -20,135.62, -20,148.52, -20,142.29, and -20,138.44 kcal/mol, for NA-LA, NA-OS, NA-PE, and NA-ZA, respectively.

3.3. Heating Dynamics Simulation

Heating dynamics simulation was executed to increase the temperature of system from 0 into 300 K. The system temperature was increased from 0 to 300 K in the first 2.5 ps then fluctuated slowly. The total energies of NA-LA, NA-OS, NA-PE, and NA-ZA complexes rose as much as kinetics energies which in range 4431-4539 kcal/mol. The trajectories stored were analyzed to get insight the NA-inhibitors interaction. The trajectories contain the data of simulated molecule.

The binding energies were calculated in vacuum through all trajectories recorded. The free binding energy could determine the ability of enzyme to bind the substrate [50-51]. For each NA-LA, NA-OS, NA-PE, and NA-ZA free binding energies are -215.67, -103.65, -116.56, and -239.34 kcal/mol respectively. The results show that NA-ZA and NA-LA complexes have lower energies than NA-OS and NA-PE complexes. This is in accordance with other results in this current study that OS and PE have less strength in binding with Indonesian H274Y mutant.

3.3.1. Inhibitors Movement during Simulation

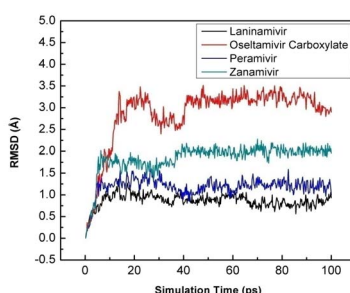


Fig. 1: The RMSD of four inhibitors during the simulation.

The stability of inhibitors was monitored by its movement during the simulation. The movement of the inhibitors while bound in the active site of NA represented by its RMSD. The RMSD of four inhibitors were plotted in Fig. 1. The RMSD of all inhibitors show that the movement of OS in the active site is relatively high. The fluctuation of OS RMSD almost surpassing 3.5 Å and being the highest value compared with LA, ZA, and PE. The ZA RMSD fluctuation is higher than PE. This is happened may be caused that since the minimization process, PE was moving away from NA active site. The number of hydrogen bonds between NA-PE was known decreased after minimization energy had been executed. The LA following with RMSD fluctuates below 1 Å.

3.3.2. Percentage of Hydrogen Bonds Occupancy

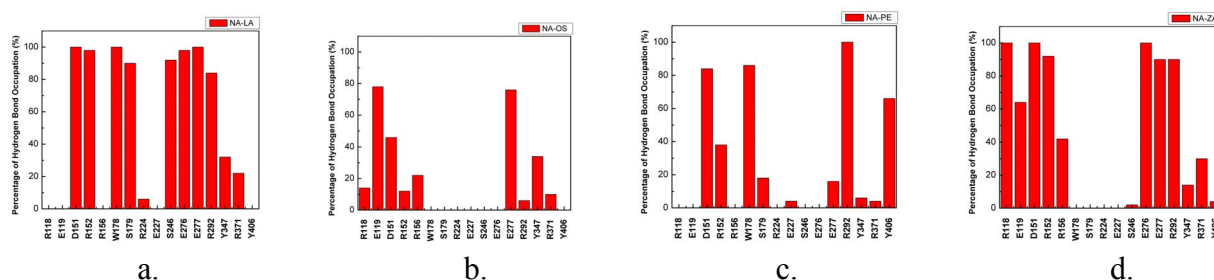


Fig. 2: The percentage of hydrogen bond occupancy of: a. NA-LA complex; b. NA-OS complex; c. NA-PE complex; d. NA-ZA complex

The interaction between NA and its inhibitors could be examined from the hydrogen bonds formed. The better interaction will result in more hydrogen bonds created between them. The strength of hydrogen bond had been monitored from its occupancy in every conformation in the trajectories. Strong hydrogen bond should have percentage of occupancy larger than 80% [52]. In Fig. 2a, 2b, 2c, and 2d, were plotted the percentage of hydrogen bond occupancy between NA and its inhibitors during the simulation. The residues will be discussed based on Stoll et al. [53] characterization with the addition of E277 into S5.

The hydrogen bond occupancy of NA-LA is shown in Fig. 2a. There are eight NA residues which produced strong hydrogen bonds with LA. In the S1 subsite, the hydrogen bond occupation was dominated by R292. Other residues, R118 and R371, did not give a big contribution into NA-LA binding. Even R118 does not make any hydrogen bond during simulation. The most contribution of bindings is come from S3 and S5 subsites residues. They are W178, S179, S246, E276, and E277 which produced the percentage of occupancy above 80%.

The percentage of hydrogen bond occupancy shown in the Fig. 2b revealed the lack of interaction between NA-OS. All functional residues have a weak interaction during simulation because all of hydrogen bond occupation percentages are below 80%. There are only two residues from S2 subsite, E119 and E227, which almost 80%. Even the NA-PE interaction is better than NA-OS. It could be observed from the three strong hydrogen bonds formed during the simulation as shown in Fig. 2c. In NA-PE interaction, the hydrogen bond bindings were dominated by D151, W178, and R292.

In Fig. 2d, the interaction between NA-ZA was revealed. The percentage of hydrogen bond above 80% were made by S1, S3 and S5 subsites residues such as R118, R152, E276, E277, R292, and catalytic residue D151. In the S1, similar with the interaction between NA-LA, R371 did not give much contribution to the bindings. While in the S3 subsite, a hydrogen bond formed only by R152, the interaction in S5 subsite of NA-ZA complex have a similarity with what happened in the NA-LA complex, the E276 and E277 have a good interaction with ZA.

4. Discussion

The main objective of this study is to compare the interaction with its inhibitors. To achieve that, we generated models, select the best model through the combination of three different assessment methods, docking the inhibitors into NA enzyme, executed minimization energy, and performed heating dynamics

simulation. The combination of three different assessment used give a comprehensive approaching to select the best model since every method used has its own specialty. Molecular docking is able to attach inhibitors into the NA enzyme. The minimization energy could optimize the molecule structure before simulated. And the last but not least, the heating dynamics simulation could be used in depth analyses of structure, energy, and electrostatic interaction of the inhibitors with the NA.

Comparison of inhibitors movement indicated that there is a difference in inhibitor response to the NA. The result of inhibitors RMSD shows that the highest movement is made by OS while the smallest is LA. As far as RMSD comparison is concerned, the findings acquired here is in line with multiple studies that infers how higher substrate RMSD suggest superior NA ability to reject an inhibitor [54-56]. Thus, the Indonesian H274Y mutant NA could be said as one of many OS-resistant.

There are a few differences in the hydrogen bond contribution between each inhibitor. The carboxylic group that acts as a “main attraction”, particularly for the 118-292-371 triad that initiates binding is observed to have two residues, R118 and R292, with strong hydrogen bonds only happens in NA-ZA. In contrast to that, NA-LA and NA-PE only had one residue, R292, which has formed strong hydrogen bonds for that exact same region while in NA-OS no residue form a strong hydrogen bonds. The strong hydrogen bond at R292 emphasizes the importance of this residue in NA-inhibitors binding. There are studies that describe inhibitor resistance caused by the R292K mutation [09-11].

Accordance with Le et al. and Maki Kiso et al. studies [21, 23], our results shows that OS-resistant variants which possess a histidine-to-tyrosine substitution at position 274 (H274Y) and an asparagine-to-serine substitution at position 294 (N294S) in NA was reduced by R-125489 (LA compound) and ZA, but not by OS. Other OS-resistant experiment shows that OS IC₅₀ ratios of 32 to 8400 for H274Y H1N1, R292K, E119K, and N294S (H3N2) mutants, while for LA and ZA are 0.69 to 2.8, and 0.72 to 1.7, respectively [22]. The values of IC₅₀ indicate that the ability of NA to bind both LA and ZA is better than OS.

5. Conclusions

This research shows a comparison of models using the combination of three different assessment methods, four inhibitors (ZA, LA, OS, and PE) affinities when attached into and simulated with NA. The unique perspective of each assessment method were used in this study have its own advantages when being worked to selecting the best model. The preferably good structure chosen is model 3 which have the best rank in verify-3D and DOPE scores and shared the 1st rank with model 4. The model which was docked with four inhibitors and simulated model shows different binding affinities. The hydrogen bonds and interaction energy shows that ZA and LA is preferable to treat a patient which infected with OS-resistant virus.

6. Acknowledgements

We would like to express gratitude towards Ding Ming Chee of Accelrys Singapore for the Accelrys Discovery Studio 2.1 trial sent to us.

7. References

- [1] WHO. H5N1 avian influenza: Timeline of major events. 2011. http://www.who.int/influenza/human_animal_interface/avian_influenza/H5N1_avian_influenza_update.pdf
- [2] E.R. Sedyaningsih, S. Isfandari, S. Soendoro, S.F. Supari. Towards Mutual Trust, Transparency and Equity in Virus Sharing Mechanism: The Avian Influenza Case of Indonesia. *Ann. Acad. Med.* Singapore 2008, **37**:482-488.
- [3] WHO. Cumulative number of confirmed human cases for avian influenza A H5N1 reported to WHO, 2003-2011. 2011. http://www.who.int/influenza/human_animal_interface/EN_GIP_20111010CumulativeNumberH5N1cases.pdf
- [4] T. Werner, and T.C. Harder. Chapter 2: Avian Influenza. Influenza Report 2006, edited by Kamps et al. *Flying Publisher* 2006, 48-86.
- [5] H. Chen, G. Deng, Z. Li, et al. The evolution of H5N1 influenza viruses in ducks in southern China. *Proc. Natl. Acad. Sci.* 2004, **101**: 10452-10457.

- [6] G. Behrens, and M. Stoll. Chapter 4: Pathogenesis and Immunology. Influenza Report 2006, edited by Kamps et al. *Flying Publisher* 2006, 92-109.
- [7] A.C. Lowen, P. Palese. Influenza Virus Transmission: Basic Science and Implications for the Use of Antiviral Drugs During a Pandemic. *Infectious Disorders - Drug Targets* 2007, **7**, 318-328.
- [8] L.J. Mitnaul, M.N. Matrosovich, M.R. Castrucci, A.B. Tuzikov, N.V. Bovin, D. Kobasa, Y. Kawaoka. Balanced Hemagglutinin and Neuraminidase Activities Are Critical for Efficient Replication of Influenza A Virus. *Journal of Virology* 2000, **74**: 6015–6020.
- [9] R.J. Russell, L.F. Haire, D.J. Stevens, P.J. Collins, Y.P. Lin, G.M. Blackburn, A.J. Hay, S.J. Gamblin, J.J. Skehel JJ. The structure of H5N1 avian influenza neuraminidase suggests new opportunities for drug design. *Nature* 2006, **443**: 45-49.
- [10] R. Chachra, R.C. Rizzo. Origins of Resistance Conferred by the R292K Neuraminidase Mutation via Molecular Dynamics and Free Energy Calculations. *Journal of Chemical Theory and Computation* 2008, **4**: 1526-1540.
- [11] J.L. McKimm-Breschkin, A. Sahasrabudhe, T.J. Blick, M. McDonald, P.M. Colman, G.J. Hart, R.C. Bethell, J.N. Varghese. Mutations in a conserved residue in the influenza virus neuraminidase active site decreases sensitivity to Neu5Ac2en derivatives. *J. Virol.* 1998, **72**:2456–2462.
- [12] V.P. Mishin, F.G. Hayden, and L.V. Gubareva. Susceptibilities of Antiviral-Resistant Influenza Viruses to Novel Neuraminidase Inhibitors. *Antimicrobial Agents and Chemotherapy* 2005, **49**: 4515-4520.
- [13] T.G. Sheu, V.M. Deyde, M. Okomo-Adhiambo, R.J. Garten, X. Xu, R.A. Bright, E.N. Butler, T.R. Wallis, A.I. Klimov, and L.V. Gubareva. Surveillance for Neuraminidase Inhibitor Resistance among Human Influenza A and B Viruses Circulating Worldwide from 2004 to 2008. *Antimicrobial Agents and Chemotherapy* 2008, **52**: 3284-3292.
- [14] N.T. Wetherall, T. Trivedi, J. Zeller, C. Hodges-Savola, J.L. McKimm-Breschkin, M. Zambon, and F.G. Hayden. Evaluation of neuraminidase enzyme assays using different substrates to measure susceptibility of influenza clinical isolates to neuraminidase inhibitors: report of the neuraminidase inhibitor susceptibility network. *Journal of Clinical Microbiology* 2003, **41**: 742-750.
- [15] J.L. McKimm-Breschkin, T. Trivedi, A. Hampson, A. Hay, A. Klimov, M. Tashiro, F. Hayden, and M. Zambon. Neuraminidase Sequence Analysis and Susceptibilities of Influenza Virus Clinical Isolates to Zanamivir and Oseltamivir. *Antimicrobial Agents and Chemotherapy* 2003, **47**: 2264-2272.
- [16] H. Yen, N.A. Ilyushina, R. Salomon, E. Hoffmann, R.G. Webster, and E.A. Govorkova. Neuraminidase Inhibitor-Resistant Recombinant A/Vietnam/1203/04 (H5N1) Influenza Viruses Retain Their Replication Efficiency and Pathogenicity In Vitro and In Vivo. *Journal of Virology* 2007, **81**: 12418-12426.
- [17] A. Meijer, A. Lackenby, O. Hungnes, B. Lina, S. van der Werf, B. Schweiger, M. Opp, J. Paget, J. van de Kasstele, J. Hay, and M. Zambon. Oseltamivir-Resistant Influenza Virus A (H1N1), Europe, 2007–08 Season. *Emerging Infectious Diseases* 2009, **15**: 552-560.
- [18] A.S. Monto, J.L. McKimm-Breschkin, C. Macken, A.W. Hampson, A. Hay, A. Klimov, M. Tashiro, R.G. Webster, M. Aymard, F.G. Hayden, and M. Zambon. Detection of Influenza Viruses Resistant to Neuraminidase Inhibitors in Global Surveillance during the First 3 Years of Their Use. *Antimicrobial Agents and Chemotherapy* 2006, **50**: 2395-2402.
- [19] D. Tamura, K. Mitamura, M. Yamazaki, M. Fujino, M. Nirasawa, K. Kimura, M. Kiso, H. Shimizu, C. Kawakami, S. Hiroi, S. Takahashi, M. Hata, H. Minagawa, Y. Kimura, S. Kaneda, S. Sugita, T. Horimoto, N. Sugaya, and Y. Kawaoka. Oseltamivir-Resistant Influenza A Viruses Circulating in Japan. *Journal of Clinical Microbiology* 2009, **47**: 1424-1427.
- [20] P.J. Collins, L.F. Haire, Y.P. Lin, J. Liu, R.J. Russell, P.A. Walker, J.J. Skehel, S.R. Martin, A.J. Hay, S.J. Gamblin, Crystal structures of oseltamivir-resistant influenza virus neuraminidase mutants. *Nature* 2008, **453**: 1258–1261
- [21] Q.M. Le, M. Kiso, K. Someya, Y. T. Sakai, T. H. Nguyen, K. H. L. Nguyen, N. D. Pham, H. H. Ngyen, S. Yamada, Y. Muramoto, T. Horimoto, A. Takada, H. Goto, T. Suzuki, Y. Suzuki, and Y. Kawaoka. Avian flu: isolation of drug-resistant H5N1 virus. *Nature* 2005, 437:1108.

- [22] M. Yamashita, T. Tomozawa, M. Kakuta, A. Tokumitsu, H. Nasu, and S. Kubo. CS-8958, a Prodrug of the New Neuraminidase Inhibitor R-125489, Shows Long-Acting Anti-Influenza Virus Activity. *ANTIMICROBIAL AGENTS AND CHEMOTHERAPY* 2009, **53**(1): 186–192.
- [23] M. Kiso, S. Kubo, M. Ozawa, Q.M. Le, C.A. Nidom, et al. Efficacy of the New Neuraminidase Inhibitor CS-8958 against H5N1 Influenza Viruses. *PloS Pathog.* 2001, **6**(2): 1-10.
- [24] <http://www.ncbi.nlm.nih.gov/genomes/FLU/Database/nph-select.cgi?go=database>
- [25] S.F. Altschul, T.L. Madden, A.A. Schaffer, J. Zhang, Z. Zhang, W. Miller, and D.J. Lipman. Gapped BLAST and PSI-BLAST: a new generation of protein database search programs. *Nucleic Acids Res.* 1997, **25**: 3389-3402.
- [26] E.M. Zdobnov, and R. Apweiler. InterProScan - an integration platform for the signature-recognition methods in InterPro. *Bioinformatics* 2001, **17**: 847-848.
- [27] K. Arnold, L. Bordoli, J. Kopp, and T. Schwede. The SWISS-MODEL Workspace: A web-based environment for protein structure homology modelling. *Bioinformatics* 2006, **22**:195-201.
- [28] F. Kiefer, K. Arnold, M. Künzli, L. Bordoli, T. Schwede T. The SWISS-MODEL Repository and associated resources. *Nucleic Acids Research* 2009, **37**: D387-D392.
- [29] T. Schwede, J. Kopp, N. Guex, and M.C. Peitsch. SWISS-MODEL: an automated protein homology-modeling server. *Nucleic Acids Research* 2003, **31**: 3381-3385.
- [30] N. Guex, and M.C. Peitsch. SWISS-MODEL and the Swiss-PdbViewer: An environment for comparative protein modelling. *Electrophoresis* 1997, **18**: 2714-2723.
- [31] M.C. Peitsch. Protein modeling by E-mail. *BioTechnology* 1983, **13**: 658-660.
- [32] <http://www.pdb.org/pdb/home/home.do>
- [33] A. Sali, L. Pottertone, F. Yuan, H. van Vlijmen, M. Karplus. Evaluation of comparative protein modeling by MODELLER. *Proteins* 1995, **23**: 318-326.
- [34] M.-Y. Shen, and A. Sali. Statistical potential for assessment and prediction of protein structures. *Protein Science* 2006, **15**: 2507-2524.
- [35] R. Lüthy, J.U. Bowie, D. Eisenberg. Assessment of protein models with three-dimensional profiles. *Nature* 1992, **356**: 83-85.
- [36] G.N. Ramachandran, C. Ramakrishnan, V. Sasisekharan. *Mol. Biol.* 1963, **7**: 95
- [37] W. Kabsch, C. Sander. Biopolymers Dictionary of protein secondary structure: Pattern recognition of hydrogen-bonded and geometrical features. *Biopolymers* 1983, **22**: 2577-2637.
- [38] R.K. Fiser, and A. Sali. Modeling of loops in protein structures. *Protein Science* 2000, **9**: 1753-1773.
- [39] R.A. Laskowski, M.W. MacArthur, D.S. Moss, and J.M. Thornton. PROCHECK - a program to check the stereochemical quality of protein structures. *Journal of Applied Crystallography* 1993, **26**: 283-291.
- [40] A.L. Morris, M.W. MacArthur, E.G. Hutchinson, and J.M. Thornton. Stereochemical quality of protein structure coordinates. *Proteins: Structure, Function, and Bioinformatics* 1992, **12**: 345-364.
- [41] <http://pubchem.ncbi.nlm.nih.gov/>
- [42] G. Wu, D.H. Robertson, C.L. Brooks III, M. Vieth. Detailed Analysis of Grid-Based Molecular Docking: A Case Study of CDOCKER - A CHARMM-Based MD Docking Algorithm. *J. Comp. Chem.* 2003, **24**: 1549-1562.
- [43] B.R. Brooks, R.E. Bruccoleri, B.D. Olafson, D.J. States, S. Swaminathan, and M. Karplus. CHARMM: A program for macromolecular energy minimization and dynamics calculations. *J. Comput. Chem.* 1983, **4**: 187–217.
- [44] Brooks et al. CHARMM: The Biomolecular Simulation Program. *J. Comput. Chem.* 2009, **30**: 1545–1614.
- [45] M.S. Lee, M. Feig, F.R. Salsbury Jr., C.L. Brooks III. New analytic approximation to the standard molecular volume definition and its application to generalized Born calculations. *J. Comput. Chem.* 2003, **24**: 1348-1356.
- [46] J.P. Ryckaert, G. Ciccotti, H.J.C. Berendsen. Numerical integration of the Cartesian equations of motion of a system with constraints: molecular dynamics of n-alkanes. *J. Comput. Phys.* 1977, **23**: 327-341.
- [47] C.L. Brooks III, B.M. Pettit, and M. Karplus. Structural and energetic effects of truncating long ranged interactions in ionic and polar fluids. *J. Chem. Phys.* 1985, **83**: 5897–5908.

- [48] P.J. Steinbach, and B.R. Brooks. New spherical-cutoff methods for long-range forces in macromolecular simulation. *J. Comput. Chem.* 1994, **15**: 667–683.
- [49] A.R. Leach. *Molecular Modelling: Principles and Applications*. 2nd Edition. *Prentice Hall* 2001: 165-181.
- [50] P. Decha, T. Rungrotmongkol, P. Intharathep, M. Malaisree, O. Aruksakunwong, C. Laohpongspaisan, V. Parasuk, P. Sompornpisut, S. Pianwanit, S. Kokpol, and S. Hannongbua. Source of High Pathogenicity of an Avian Influenza Virus H5N1: Why H5 Is Better Cleaved by Furin. *Biophysical Journal* 2008, **95**: 128–134.
- [51] X.L. Guo, D.Q. Wei, Y.S. Zhul, and K.C. Chou. Cleavage mechanism of the H5N1 hemagglutinin by trypsin and furin. *Amino Acids* 2008, **35**(2): 375-382.
- [52] M. Shu, Z. Lin, Y. Zhang, Y. Wu, H. Mei, and Y. Jiang. Molecular dynamics simulation of oseltamivir resistance in neuraminidase of avian influenza H5N1 virus. *J Mol Model* 2010.
- [53] V. Stoll, K.D. Stewart, C.J. Maring, S. Muchmore, V. Giranda, Y.-g.Y. Gu, G. Wang, Y. Chen, M. Sun, C. Zhao, A.L. Kennedy, D.L. Madigan, Y. Xu, A. Saldivar, W. Kati, G. Laver, T. Sowin, H.L. Sham, J. Greer, D. Kempf. Influenza Neuraminidase Inhibitors: Structure-Based Design of a Novel Inhibitor Series. *Biochemistry* 2003, **42**: 718-727.
- [54] O. Aruksakunwong, M. Malisree, P. Decha, P. Sompornpisut, V. Parasuk, S. Pianwanit, and S. Hannongbua. On the Lower Susceptibility of Oseltamivir to Influenza Neuraminidase Subtype than Those in N2 and N9. *Biophysical Journal* 2007, **92**: 798-807.
- [55] L. Le, E. Lee, K. Schulten, and T.N. Truong. Molecular Modeling of swine influenza A/H1N1, Spanish H1N1, and avian H5N1 flu N1 Neuraminidase bound to Tamiflu and Relenza. *PloS Current Beta* 2009.
- [56] J. Gong, W. Xu, and J. Zhang. Structure and Functions of Influenza Virus Neuraminidase. *Current Medicinal Chemistry* 2007, **14**: 113-122.